Acta Materialia 150 (2018) 394–402

Contents lists available at ScienceDirect

Acta Materialia

journal homepage: www.elsevier.com/locate/actamat

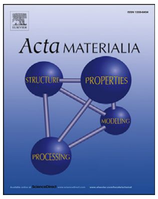

Full length article

Kinetics and thermodynamics of densification and grain growth: Insights from lanthanum doped zirconia

Hui Li, Sanchita Dey, Ricardo H.R. Castro*

Department of Materials Science and Engineering, University of California-Davis, CA 95616, United States

ARTICLE INFO

Article history:
Received 8 December 2017
Received in revised form
20 February 2018
Accepted 19 March 2018
Available online 22 March 2018

Keywords:
Sintering
Grain growth
Calorimetry
Ceramics
Oxides

ABSTRACT

The effect of dopants (or additives) on sintering is typically addressed from a mechanistic and diffusivity perspective by focusing on how dopants affect those parameters. However, a comprehensive description of sintering needs to address the role of dopants in the thermodynamics of the system, which affects local chemical potentials driving forces and is, therefore, ultimately linked to the mass transport mechanisms themselves by the thermodynamic extremal principle. In this work, Lanthanum doped Yttria-Stabilized-Zirconia (YSZ) sintering was studied from both kinetics and thermodynamic perspectives to demonstrate the need for those complementary analyses to allow proper processing control. La caused inhibition of both grain growth and densification, which was a result of a change of interfacial energies linked to La segregation as well as of the codependence of coarsening and densification on the grain boundary energy. While La caused a modest decrease in the activation energy for densification, surface and grain boundary energies decreased from 0.95 to 0.70 J/m^2, respectively, for YSZ, to 0.80 and 0.41 J/m^2 for 2 mol% La-YSZ, indicating an increase in sintering stress. The apparent contradiction between the thermodynamic data and the observed densification trend is attributed to the reduced grain growth that trapped the system in a metastable configuration.

1. Introduction

Thermally activated grain growth can severely limit operation of nanocrystalline materials under high temperature environments and even moderate processing conditions. This tendency to grain coarsening is attributed to the high excess energy stored in the material in the form of interfaces, which under conditions of high diffusivity will be eliminated to form the less energetic bulk counterpart [1]. The kinetics of grain growth can be expressed by the general equation [2]:

$$v = \frac{dD}{dt} = M_{gb}\frac{\gamma_{gb}}{D} \tag{1}$$

where v is the velocity of grain boundary (GB) migration, M_{gb} is the GB mobility, γ_{gb} the GB energy, and D is the average grain size. A potential method to retard the grain growth is to target a decrease in either GB energy and/or mobility [3]. Lanthanum has been shown to cause resistance to grain growth in cubic zirconia [4]. From a kinetic perspective, lanthanum segregation to the boundaries can reduce boundary migration by pinning. Such effect of dopants on the mobility of boundaries has been addressed in several ceramic systems, such as yttria and ceria [5–7]. On the other hand, from an energetic perspective, the grain growth inhibition is also related to reduction of the average GB energies [4] resulting from segregation according to an extension of the Gibbs adsorption isotherm expressed in Eq. (2) [8].

$$\gamma_{gb} = \gamma_0 - \Gamma_B\left(RTlnX_B^{bulk} - \varDelta H_{seg}\right) \tag{2}$$

Here, γ_0 represents the original GB energy without dopant segregation, Γ_B is the excess of dopant at the boundary, $\varDelta H_{seg}$ is the segregation enthalpy of dopants, and X_B^{bulk} is the dopant content dissolved in the bulk. Although this equation is here written for GBs, analogous equations can also be written for surfaces [9]. Therefore, in systems where both surfaces and grain boundaries are present, dopants will affect both, and consequently influence driving forces for microstructural evolutions accordingly [10,11].

Lange et al. [12,13] has theoretically addressed the importance of interface energies in sintering by using geometric models to demonstrate that the changes in dihedral (equilibrium) angles

---

* Corresponding author.
E-mail address: rhrcastro@ucdavis.edu (R.H.R. Castro).

https://doi.org/10.1016/j.actamat.2018.03.033
1359-6454/

affect the sintering “stress”, i.e. the energy difference between the equilibrium condition and the non-sintered (or partially sintered) particles [14]. In theory, large dihedral angles would be linked to high sintering stresses (potentially causing more densification) as compared to small dihedral angles; or in other words, the lower the ratio of grain boundary energy to surface energy is, the stronger the tendency to densification in both early and late stages of sintering [15]. Lange suggests that although the dihedral angle is an ‘equilibrium’ condition, this state is met frequently during sintering as the neck growth occurs in between particles. Once met, a particulate system can only exit this metastable condition if coarsening occurs, leading to a consequent change in the contact angle, as noted in experimental data in the literature [12]. This connection between the density and the grain size was later formalized by Castro and Gouvea [16]:

$$\left(\frac{1}{\rho}-\frac{1}{\rho_0}\right)=\frac{6V}{P}\left(\gamma_S\frac{dA_P^{GC}}{dA_T}-\gamma_{gb}\frac{dA_{GB}}{dA_T}\right)\left(\frac{1}{D}-\frac{1}{D_0}\right) \tag{3}$$

Here, dA_{GB} is the grain boundary area change, dA_P^{GC} is the contribution for pore elimination coming from grain coarsening, ρ is the density of the sintered part and ρ_0 is the initial density, and D and D_0 are the respective grain sizes. γ_S is surface energy, A_P the surface area, A_{GB} grain boundary area, A_T is the total interfacial area including, pore surfaces and grain boundaries, P is the external pressure and V is the molar volume. This equation suggests grain growth is actually a requirement for densification although the extent of needed grain growth is specific for each system and determined by the multiplier factor in Eq. (3). Surprisingly, when plotting $\left(\frac{1}{\rho}-\frac{1}{\rho_0}\right)$ versus $\left(\frac{1}{D}-\frac{1}{D_0}\right)$ with sintering data available in the literature, it is not uncommon to observe a linear behavior. This suggests that the multiplying term in Eq. (3) is the (constant) slope of the line, representing how much density changes as a function of grain size.

Despite the existence of this description of the role of interfacial energies in sintering and the parallel work on the effect of dopants on interfacial energies themselves, the impact of dopants on the thermodynamics of sintering is typically disregarded as relevant. Dopants are only considered to affect mechanisms of sintering, causing densification or not depending on which mechanism is (de) activated [17]. Although the mechanisms have their driving force attributed to the curvature forces alone [18], from the optics of the thermodynamic extremal principle, it is safe to say that sintering stress and mechanisms must be intimately connected. That is, the changes in chemical potential caused by dopant segregation to interfaces will be the actual driving forces for changes in mass transport mechanisms by defining the path of maximum energy dissipation. This perspective is aligned with recent reports demonstrating interfacial energies are more relevant driving forces in sintering than the neck curvature [19]. Chang et al. demonstrated that de-sintering, i.e. pore volume increase, can be induced in SnO_2 if the dihedral angle is purposely modified by changing interfacial energies, causing mass flow against the neck curvature.

Here we study the sintering of lanthanum-doped cubic zirconia from both conventional kinetics and thermodynamics perspectives in an attempt to build more solid database to better understand the connections between those theories. Previous literature shows evidences of La segregation to grain boundaries in yttria-stabilized cubic zirconia [4], which leads to grain boundary energy reduction and a resultant coarsening inhibition. However, similarly to rare-earth segregation in spinel structures [20] it is likely that the observed segregation is also occurring at surfaces, affecting this energy and consequently the dihedral angle. The results presents here demonstrate lanthanum inhibits grain boundary velocity while changing the ratio between interfacial energies, which increase the dihedral angle and therefore the sintering stress. Contradictorily, despite the quantified increase in densification driving force, the strong coarsening inhibition traps the system in a metastable state with relatively low density.

2. Experimental procedures

2.1. Powder synthesis

Co-precipitation method was used to prepare both 10 mol% Y doped ZrO_2 (10YSZ) and La-doped 10YSZ nanoparticles (1 and 2 mol% La + 99 or 98 mol% 10YSZ). Zirconium (IV) oxynitrate hydrate (Sigma-Aldrich, 99%), yttrium (III) nitrate hexahydrate (Alfa Aesar, 99.999%), and lanthanum (III) nitrate tetrahydrate (Acros, 99.9%) were used as cationic precursors, and dissolved into deionized water (D.I. water) in the appropriate molar fraction. Three times excess of ammonium hydroxide as compared to stoichiometric amount for the expected precipitation reaction were used for the cationic solution to be dripped into for hydroxide precipitation. Very small hydroxide precipitates were formed during this reaction as a result of the supersaturation caused by the excess. The powder was then washed three times with anhydrous ethanol. Hydroxide precipitates were separated by centrifugation and dried at 90 °C for 48 h. Finally, after calcination in box furnace at 450 °C for 2 h, nano-scale oxide nanoparticles were obtained.

2.2. Sintering studies

Fast firing was used for sintering studies in this work [21–23]. Uniaxial pressing at 50 MPa followed by Cold Isostatic Pressing (CIP) (CIP-20TZ, MTI Corporation) at 300 MPa was used to prepare 10 mm diameter pellets. Green relative densities of pressed pellets were measured to be 35.31 ± 0.11% by geometrical estimates (samples were too fragile for Archimedes' immersion method). Pellets are pre-heated at around 500 °C for 1 min at the marginal region of firing tube (Lindberg blue. M, Thermo scientific), and then rapidly inserted into the central high temperature isothermal region for final sintering with a heating rate estimated at 700 °C/min. Samples were sintered at 1100°C-1300 °C (central temperature) for various times and were removed and quenched into air within 30s in order to capture the temporal state of the microstructure.

2.3. Characterization of powders and sintered samples

X-ray diffraction (XRD) patterns using a Bruker-AXS D8 Advance X-ray diffractometer (Bruker AXS Inc. Madison, USA) with Cu $K\alpha$ radiation ($\lambda = 1.5406$ Å) (accelerating voltage of 40 kV and an emission current of 40 mA) were collected to characterized the synthesized nanoparticles and sintered pellets, for crystallite size, phase and crystalline structure. Grain size was calculated using whole profile fitting in JADE 6.1 (MDI) software. Surface areas were measured by Brunauer– Emmett–Teller (BET) method with nitrogen adsorption (Micromeritics Gemini VII), and density of the sintered pellets were measured by Archimedes' method. Relative density (RD), which was the ratio of experimental density and theoretical density (ρ_T) determined from the measured lattice parameters determined by XRD, was used to determine the degree of densification. Fracture surfaces of sintered pellets were observed using scanning electron microscopy (SEM) (FEI 430 Nano-SEM instrument, FEI Company, Hillsboro, Oregon) to analyze grain sizes and microstructure. Line intercept method was used for analyzing grain size of samples after sintering in ImageJ software, averaging from at least 300 grains for each sample.